Talanta 224 (2021) 121927

Contents lists available at ScienceDirect

Talanta

journal homepage: www.elsevier.com/locate/talanta

Phosphorescent palladium-tetrabenzoporphyrin indicators for immunosensing of small molecules with a novel optical device

Arik Monash [a], Daniele Marciano [b,**], Arthur (Skip) Colvin [c], Rafi Fass [c,***], Yair Dvash [c], Osnat Rosen [a,*]

[a] Department of Biotechnology, Israel Institute for Biological Research, Ness Ziona, 7410001, Israel
[b] Department of Organic Chemistry, Israel Institute for Biological Research, Ness Ziona, 7410001, Israel
[c] Ryshens, LTD, Israel

ARTICLE INFO

Keywords:
Indicator displacement assay (IDA)
Optical biosensor
Immunosensor
Palladium-tetrabenzoporphyrins
Estradiol
Small molecules

ABSTRACT

Small-molecule detection is important for many applications including clinical diagnostics, drug discovery, environmental screening, and food technology. Current techniques suffer from various limitations including cost, complex sample processing, massive instrumentation, and need for expertise. To overcome these limitations, a new optical immunosensing assay for the detection of small molecules was developed and assessed with the targets estrone (E1) and estradiol (E2). For this purpose, phosphorescent indicators were designed based on the tetrabenzoporphyrin skeleton directly linked to E1 or E2, or attached through a linker, with phosphorescence lifetimes in the range of ~100–~300 μs. The assay is an indicator displacement assay (IDA). The best performances of our optical immunosensor were obtained with the indicators E1-L-Por and E2-L-Por. As they bound to specific polyclonal antibodies, their phosphorescence (τ ~200 μs) was quenched. When an endogenous competitor was added, the indicator was displaced, and the phosphorescence was immediately recovered. These effects were measured with a new optical device, described here, and able to detect picograms of luminescent molecules emitting in the NIR range, simply by measuring phosphorescence decay. This radical switch-off/switch on process demonstrates that E1-L-Por and E2-L-Por are good candidates for *in vivo* and *in vitro* immunosensing of E1 and E2. Importantly, the present immunosensing assay can be easily adapted to other small molecules such as other hormones and drugs.

1. Introduction

Detection of small molecules (<1000 Da) which have a variety of biological, pharmacological, or environmental functions, is important in the fields of molecular biology, environmental screening, medicine, and food technology. They may be contaminants, toxins, teratogens, immunodepressants, and may be lethal. For those reasons, efforts have been made to develop new methods to detect small molecules even in trace amount [1–3]. Detection is challenging due to the difficulty in recognizing them, especially in complex samples. Many are detected by highly sensitive and specific chromatographic methods [4]; however, these methods are very expensive, and require substantial instrumentation and expertise. Other bioanalytical detection methods include lateral flow assays, enzyme-linked immunosorbent assays (ELISAs), microarrays and fluorescent electrochemical sensors [5,6] Compared to these classical methods, use of biosensors has several advantages, including high specificity, reduced sample manipulation, minimal solvent volume, and easy portability. For these reasons, biosensors offer a cheap, fast, and uncomplicated alternative [7].

A biosensor is an analytical device that provides an output signal related to the concentration of a target analyte in a sample. Affinity biosensors are based on specific biorecognition elements which can bind to the analytes. The signal generated is proportional to the amount of target analyte in a specific reaction. Surface plasmon resonance (SPR) is an optical signal-transducer allowing real-time monitoring of label-free biomolecular interactions [8,9]. Other label-free detection technologies like antibody based SPR enhanced or not by nanoparticles [10–15], enzyme based SPR [16,17], surface-enhanced Raman spectroscopy

* Corresponding author.
** Corresponding author.
*** Corresponding author.
E-mail addresses: daniele@iibr.gov.il (D. Marciano), rafi@ryshens.com (R. Fass), osnatr@iibr.gov.il (O. Rosen).

https://doi.org/10.1016/j.talanta.2020.121927
Received 18 October 2020; Received in revised form 24 November 2020; Accepted 25 November 2020
Available online 28 November 2020

(SERS) including antibody based SERS [18], aptamer-based SERS [6,19], molecular imprinted polymer (MIP)-based SERS [5,20,21], and interferometry including interferometric sensors based on aptamer [22,23], antibodies [24–28], polymers [29,30] and proteins [31] as well as electrochemical sensors (ES) [32–34] such as MIP based ES [35], aptamer based ES [36], and protein based ES [37].

Immunosensors rely on recognition of an antigen by an antibody which serves as a biorecognition element [10,38]. The extreme specificity of an antibody for a cognate antigen leads to a very stable antigen-antibody complex. Identification and quantification of the antigen may be performed by means of a suitable signal transducer attached to the antigen labeled with a chemical compound like a dye or a light-emitting chromophore. Measurement of immunosensors are based on changes in the optical characteristics of a transducer surface upon direct or indirect interaction between a labeled analyte and an antibody. The optical transducers differ by different optical properties including light absorbance, reflectance, and emission (*e.g.*, fluorescence or phosphorescence) [2]. An essential requirement for effective direct detection is that the analyte of interest produces a large enough response in a required concentration range that generates a measurable signal. Molecules with high molecular weights (protein, RNA, etc.) fit this requirement. The sandwich assay format (antibody I/analyte//antibody II) is sometimes used to improve the signal and the sensitivity. Smaller molecules (molecular weight <5000) often do not generate a sufficient signal change, requiring measurement using either competitive or inhibition detection formats [39]. One commonly used format is the indicator displacement assay (IDA) in which the indicator is first allowed to bind reversibly to a receptor (the "host") [40,41]. Then, a competitive analyte is introduced into the system causing displacement of the indicator from the host, which generates an optical signal. The affinity between the indicator and the receptor must be comparable to the affinity between the analyte and the receptor. IDA offers many advantages over traditional sensing: first, the indicator is not covalently attached to the host. Second, the same host can bind many indicators. Third, the assay can be performed in either organic or aqueous media. Finally, the assay can readily be adapted to different receptors (antibodies, aptamers, peptides and enzymes, imprinted polymers), and other platforms, for quick analysis. An important class of IDAs is the fluorescent IDA (F-IDA) which uses fluorescent indicators.

F-IDA assays were developed to identify and characterize small molecules. Examples of common fluorochromes are cyanine dyes, xanthone or thioxanthone derivatives, dye-labeled aminoglycosides, 2-aminopurine, ethidium bromide or triazole orange for the detection of ligands targeting RNA [42] or for microRNA precursors [43–45], but also bioluminescent luciferase for the detection of ATP [46], europium particles for the detection of cardiac troponin I [16], naphthoates for the detection of glyphosate [47] or anthracene and xanthene derivatives for the detection of nitric oxide, hydrogen peroxide, peroxynitrite or hypochlorous acid in oxidative cleavage reactions and hydrogen sulfide in reductive cleavage reactions [48]. In some cases, phosphorescent indicators are preferred. Phosphorescence is a process in which the energy absorbed by a substance is released by intersystem crossing from a high excited state to a lower excited state of different spin multiplicity (generally the triplet state). Triplet lifetimes are in the order of milliseconds. However, some compounds have triplet lifetimes lasting minutes or even hours. The energy is released in the form of light. Unlike with fluorescence, phosphorescent materials store absorbed energy for a longer time and re-emit the radiation up to several hours after the original excitation [49]. Pt (II) and Pd(II)-coproporphyrins I-III conjugates were found suitable as delayed luminescent labels because of their high phosphorescence quantum yield, moderate triplet lifetime, high molar extinction coefficient, and good photostability. They were developed as labels of proteins and other biomolecules in the design of sensitive bioassays based on phosphorescence and time-resolved fluorescence detection [50,51]. Phosphorescent metal dye complexes like platinum (II) or palladium (II) porphyrins absorbing in the red part of the spectrum (620–650 nm) and emitting in the near-infrared (NIR) (700–950 nm) have lately received more attention as optical oxygen sensors due to their low autofluorescence emitted naturally by a biological substance, light scattering and high tissue transparency [52,53].

Assay of estrone (E1), estradiol (E2) and other sex hormones are good examples that illustrate the importance of a rapid, sensitive, precise, and cost-effective methods for detecting small molecules [54,55]. These hormones have relevant roles in various physiological processes and large impact on the reproductive and sexual function of both women and men. In addition, the detection of estrone and estradiol is important in environmental monitoring because of their high endocrine disrupting potency and their release into water-waste following their use as synthetic hormones in animals and humans. Because estrone and estradiol are not water-soluble, they are eliminated from the body mainly as their sulfate and glucuronide metabolites [56]. Numerous methods have been developed and used for the detection of these hormones including gas chromatography [57,58], high performance liquid chromatography [59,60], voltammetry [61,62], electrochemical immunosensing [63–67], chronoamperometry [68,69], enzyme biosensors [70], DNA biosensors [71,72], radioimmunoassays [73,74], colorimetric assays [75], chemiluminescent assays [76,77] and fluoroimmunoassays [78]. For example, the synthesis of an estradiol-tetraphenylporphyrin (E2-TPP) conjugate has been described [79]. This conjugate binds with high affinity to the estrogen receptor–ligand binding domain for photodynamic therapy used in cancer treatment.

We present here a simple, novel, specific, rapid, and sensitive IDA method for detecting estrone (E1) and 17β-estradiol (E2) (Scheme 1). In this assay, the immunosensing system combines a specific antibody against E1 or E2, and a novel indicator based on tetrabenzoporphyrin that is covalently linked, directly or indirectly, to E1 or E2. These conjugates are phosphorescent in solution. When they bind to the antibody, the phosphorescence is fully quenched. When a competitive analyte (E1 or E2 sulfate, or glucuronide) is introduced into the system, it displaces the indicator from the antibody, and the recovered phosphorescence lifetime can be measured by a unique and very sensitive device. The proposed method can easily be implemented for other biological and chemical applications.

2. Materials and methods

2.1. Reagents

Estradiol glucuronide (E2G, E2127), estradiol sulfate (E2S, E9505), estrone glucuronide (E1G, E1752), estrone sulfate (E1S, E0251) (see Scheme 2) and Tween 20 were purchased from Sigma Aldrich Israel. Estradiol 6-cmo-BSA (80-IE30) was purchased from Fitzgerald. E1G-BSA (LA432) was purchase from EastCoast Bio. Immunoassay Blocking (BSA free) (ab171535) was purchased from Abcam. Rabbit anti Estradiol (E2) polyclonal antibody was purchased as a special preparation by Genescript, NJ, USA. Rabbit anti Estrone (E1) polyclonal antibody (PAB003Ge01) was purchased from Cloud-clone Corp. China. Donkey anti rabbit antibody conjugated to HRP (711-035-152) was purchased from Jackson and KPL sureblue (5120–0081) was purchased from Seracare. All the tetrabenzoporphyrins reported in this paper were designed by us and purchased from Porphychem SAS. Faculté des Sciences Mirande, 9 avenue Alain Savary, 21000 Dijon. France.

2.2. Compounds names and labels (see Scheme 2)

Pd(TPTBP-S4): Palladium (II) 5,10,15,20-(tetra-4-sulfonatophenyl) tetrabenzoporphyrin trisodium salt; **Por-COOH**: Palladium (II) 5-(4-carboxyphenyl)-10,15,20-(tri-4-sulfonatophenyl) tetrabenzoporphyrin trisodium salt; **E1-Por**: Estrone palladium (II) 5-(4-carboxyphenyl)-10,15,20-(tri-4- sulfonatophenyl) tetrabenzoporphyrin trisodium salt conjugate; **E2-Por**: Estradiol palladium (II) 5-(4-carboxyphenyl)-10,15 20-(tri-4-sulfonatophenyl) tetrabenzoporphyrin trisodium salt

conjugate; **E1-L-Por**: Estrone palladium (II) 5-(4-carboxyphenyl diethylene glycol)-10,15,20–1 (tri-4-sulfonatophenyl) tetrabenzoporphyrin trisodium salt conjugate; **E2-L-Por**: Estradiol palladium (II) 5-(4-carboxyphenyl diethylene glycol)-10,15,20–1 (tri-4-sulfonatophenyl) tetrabenzoporphyrin trisodium salt conjugate. The spectroscopic properties of these new compounds that are relevant to the present study are summarized in Table 1. Absorption and emission data as well as phosphorescence lifetime were measured at three different temperatures (25, 37, 50 °C).

2.3. The optical device

The phosphorescence decay time reader is a custom device consisting of a central microcontroller (Nordic NRF52832) using four silicon photomultiplier detectors (SiPM, On Semiconductor, MICROFC-30035-SMT-TR1) and eight excitation LEDs (Vishay Semiconductor VLMK23R1S1-GS08, 630 nm peak) all operating in unison through four optical pods arrayed at ninety degrees surrounding a polished nickel plated aluminum reflective inner sphere. The polished inner chamber is then contained within a light tight black Delrin encasement. This reader system is then connected to and powered by USB to a laptop for operation and control through a custom application. A reading is taken on command from the laptop console which then drives the LED array to pulse and the emission signal (V) is then captured by the analog to digital converter (ADC) from the four SiPM detectors at 5 μs intervals and recorded into memory for profiling the measured decay curve. The measurement data are reported on the laptop screen as both the graphical decay curve and the decay time value in microseconds.

Data samples are collected using a 12-bit ADC at a sampling interval of 5 μs. Sampling begins approximately 100 μs prior to the excitation LEDs being switched off and continues for a total of 2000 μs. A programmable-gain amplifier is positioned after the photomultiplier but prior to the ADC in the signal chain. The system attempts to keep the signal amplitude between 30% and 90% of ADC saturation, thus minimizing noise and distortion and maximizing the resulting quality of curve fit.

The decay time is calculated by correcting the sample data points for time and DC offsets, linearizing the corrected data by taking the natural log of each point, and then performing a least-squares fit over the first 125 linearized corrected data points. If fewer than 125, but at least 11, corrected data points are available, the fit is done over that reduced set. Assuming that the corrected data follows an exponential curve, the slope of the linearized corrected data equals the negative reciprocal of the time constant of that exponential curve. If the fit succeeds, regardless of the residual, the automatically calculated decay time is reported. If an insufficient number of samples is available (less than 11), a decay time of 0 μs is reported.

After the curve fitting process described is performed, and either a non-zero decay time or a zero value (indicating a fit failure) is calculated, all the parameters (decay time, DC offset, amplifier gain, and uncorrected data points) are sent to the PC. Software running on the PC then plots the uncorrected ADC data as millivolts at the ADC versus time and overlays the reported decay time (or dashes to indicate a zero value), the gain used for the measurements, and a line showing the measured DC offset.

2.4. Surface plasmon resonance assay

Binding and dissociation of the rabbit Abs anti E2 and anti E1 with estrone/estradiol derivatives and their porphyrin conjugates was monitored by surface plasmon resonance (SPR) with a BIAcore T200 apparatus (GE Healthcare Life Sciences). Abs were captured on a proteinA chip (GE Healthcare Life Sciences) with TST buffer (DDW, 8.5% NaCl, 1 M Tris, 0.05% Tween20, pH 7.6) serving as running buffer until 1,000RU was reached (flow rate 10 μL/min for 5 min). The association of the captured Abs with estradiol/estrone derivatives and their porphyrin conjugates was monitored by injecting different concentrations of the small molecules for 2 min at a flow rate of 30 μL/min. The dissociation of the small molecules from the Abs was tested by stopping their injection. Glycine 10 mM, pH 1.5 regenerated the chip to enable new capture cycles. Data Analysis: Sensograms were fitted to steady state model (T200 evaluation software). Standard errors are reported as well as X2.

2.5. Spectroscopic properties of the tetrabenzoporphyrin derivatives

The absorption and emission wavelengths of the tetrabenzoporphyrin derivatives were measured in water (6.8 mM), at different temperatures (25–50 °C), and their extinction coefficients calculated at the Soret band (~440 nm) and at the Q band (~627 nm) (see Table 1). As expected, the absorption maxima were very similar. The extinction coefficients at the Soret band were about twice that at the Q band. The relative emission intensities of these compounds at 804 nm were measured at different concentrations (0.002–0.02 mg/mL - excitation at 635 nm) (see Table 1). Calibration curves were performed as follows: 0.4 mg Por-COOH was dissolved in 20 mL DDW and absorbance measurements of serial dilutions (0.02, 0.01, 0.005 mg/mL, 200 μL for each read) were taken at 440 and 627 nm. Calibration curves were plotted as absorbance at 440 and 627 nm vs. concentration and were used for all ELISA measurements. In the same manner, calibration curves for each of the porphyrin derivatives were established. The lifetimes of all the tetrabenzoporphyrin derivatives in water (10 ng/mL) were measured between 25 and 50 °C. All the spectroscopic measurements were performed in the presence of sodium sulfite, a well-established oxygen scavenger.

2.6. Development of an indirect competitive ELISA assay

Estradiol 6-cmo-BSA or E1G-BSA were diluted in 50 mM bicarbonate buffer (pH 9.6) and 50 μL was added to each well of polystyrene microtiter 96 well (Maxisorp, NUNC) and incubated overnight at 4 °C. The amount of coating antigen that was found suitable for this assay was 2 μg/well. Wells were washed three times with 300 μL/well of wash buffer (DDW, 0.9% NaCl, 0.05% Tween20) and blocked with 250 μL/well of immunoassay blocking buffer (BSA free), followed by incubation for 1 h at 37 °C. 50 μL/well of serial dilutions of estradiol/estrone derivatives and their porphyrin conjugates in TST buffer were pre-incubated with the same volume of matching antibody (1:2000 for Rabbit anti E2, 1:10,000 for Rabbit anti E1, diluted in TST) for 1 h in a U-bottom plate at 37 °C. After 1 h, 50 μL of the pre-incubated antibody and various concentrations of estradiol/estrone derivatives and their porphyrin conjugates were added to the coated plate and incubated for 1 h at 37 °C. After washing, 50 μL/well 1:1000 of HRP-Donkey anti rabbit antibody in TST was added for 30 min at 37 °C. Finally, after washing, 50 μL/well of KPL sureblue was added and incubated for 10 min at room temperature. The enzymatic reaction was stopped by adding 100 μL/well 0.5 M H_2SO_4 and the plate was spectro-photometrically read in a single absorbance wavelength mode at 450 nm. TST buffer was used as a control in all assays. A calibration curve was fitted based on the average of at least three separate assays in duplicate. As opposed to direct ELISA in which ratio between signal to blank is measured, the data for indirect ELISA is calculated using the IC_{50} values, which represent the concentration of estradiol/estrone derivatives that produced 50% inhibition of antibody binding to the estradiol conjugate.

2.7. Quenching assay

The IDA was performed using the following steps: 500 μL of E1-L-Por or E2-L-Por was diluted in TST buffer +2% Na_2SO_3 in tubes. Then, 500 μL of matching antibody diluted in TST buffer was added to half of the tubes while TST buffer was added to the other half for control. The tubes were then incubated at 37 °C for 30 min and phosphorescence was

measured in a special device (see Sec. 2.3). After measuring, 10 μL of 2 μg/mL of a competitive analyte (E1/E2 derivative) was added following incubation for 30 min at 37 °C. Finally, the tubes were re-measured for phosphorescence.

3. Results and discussion

3.1. Molecular requirements and design

Our goal was to develop water-soluble molecules bearing an estrone (E1) or estradiol (E2) moiety (as analytes) for recognition by estrone and estradiol antibodies through the formation of analyte-specific antibody complexes. The rationale behind our synthetic design was the need to perform an IDA with porphyrin derivatives of estrone or estradiol [80], possessing long fluorescence lifetimes. These porphyrin conjugates are allowed to bind reversibly to the antibody. Their phosphorescence should be quenched as long as the porphyrin conjugate is attached to the antibody, and their phosphorescence lifetime should diminish strongly. Then, a competitive analyte, estrone or estradiol, is introduced into the system and displace the porphyrin conjugate out of the antibody active site. At this point, a strong phosphorescent emission is expected to occur as in the free labeled analyte, and the fluorescence lifetime should revert (increase) to its previous value (See Scheme 1 for illustration of the expected change in emission lifetime decay during the IDA).

To optimize the detection before and after binding to the target, the molecule must excite at 620–640 nm, emit above 700 nm, with a decay time (fluorescence lifetime) in the 50–300 μsec range (the longer the better). The photophysical properties of the estradiol-tetraphenylporphyrin (E2-TPP) conjugate [79] do not fit these requirements. Palladium tetrabenzoporphyrin (Pd-TBP) were already described as better emitting systems [81]. They absorb at 407 nm and phosphoresce at 687 nm, with a quantum yield and lifetime of Φ 7.9 and τ 0.260 msec, respectively. Organic soluble derivatives of Pd-TBP were also developed which absorb in the blue (Soret band 440–480 nm) and in the red (Q-band 620–650 nm) and show bright phosphorescence in the NIR at 742–800 nm with quantum yield up to 30%. We assumed that molecules based on the meso-tetraphenyl-substituted tetrabenzoporphyrins (TPTBP) skeleton (see Scheme 2) should be suitable and that they should fit the expected photophysical properties [82]. TPTBP exhibits an absorption band at 633 nm with a large extinction coefficient (ε 2.58 × 10^4 in toluene), and an emission band at 783 nm with modest quantum yield (Φ 0.03) and fluorescence lifetime (τ 3.9 ns in DCM or 2.8 ns in benzene). Metalation of TPTBP with palladium (II) led to a phosphorescent complex, Pd (TPBTBP) (see Scheme 2), with longer lifetime (τ 223.7 μs at 793 nm in toluene or 258 μs at 797 nm in DMA) and still modest quantum yield at 797 nm (Φ 0.08 in DMA) [83]. Sulfonation of the phenyl groups of the TPTBP produces Pd-tetrabenzo (tetraphenyl) porphyrin tetrasulfonic acid (Pd (TPTBP-S_4), see Scheme 2) having a good water solubility and high quantum efficiency at room temperature (τ 124 μs, at 800 nm in water) while maintaining the same absorption frequency at 625 nm. The Pd (TPTBP-S_4) system fits our requirements as a label for estrone and estradiol.

The more straight-forward porphyrin conjugates that we designed had their porphyrin skeleton directly covalently attached to the estrone/estradiol moieties like in E1-Por and E2-Por (see Scheme 2). The tetrabenzoporphyrin size is at least twice that of E1 or E2, so there is a probability that it will hinder the approach and the insertion of E1 or E2 inside the antibody pocket. Compounds in which an optimal distance is kept between E1 or E2 and the tetrabenzoporphyrin skeleton maybe preferred as E1 or E2 indicators. Hydrophilic linkers like mono or polyethylene glycol can be used to avoid any steric hindrance by the porphyrin multi-ring system when approaching the antibody binding site, while preserving the water-solubility of the molecule. For the synthesis of such porphyrin conjugates, the replacement of one sulfonate group in Pd (TPTBP-S_4) by a carboxyl group is necessary. A carboxylate derivative was prepared (Por-COOH) of which the carboxyl group facilitates the attachment of an estrone or estradiol molecule by direct esterification. This method yielded the first potential porphyrin derived indicators, E1-Por and E2-Por (see Scheme 2). If needed, ethylene glycol modified estrone or estradiol could be attached to the same carboxyl group yielding E1-L-Por and E2-L-Por, respectively. Relying on earlier investigations [84] we assumed that the photophysical properties would be maintained through these modifications and be similar to those of Pd (TPTBP-S_4).

Five new porphyrin derivatives were designed and used in the present studies: Por-COOH, E1-Por, E2-Por, E1-L-Por and E2-L-Por. Their structures were based on the palladium-tetraphenyltetrabenzoporphyrin skeleton. As expected, all of them

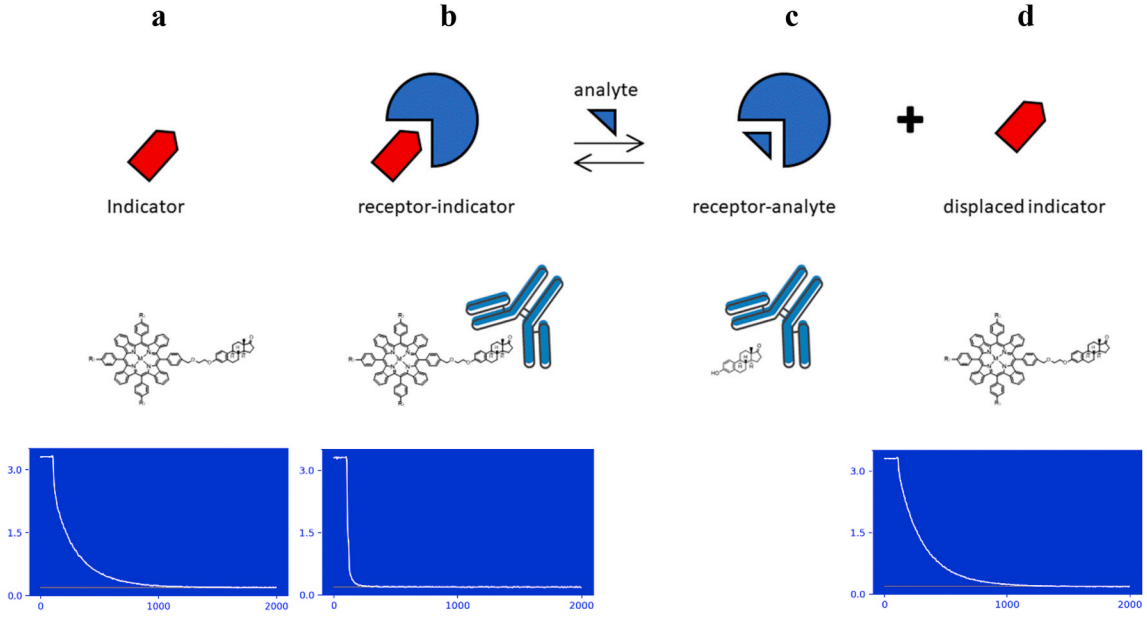

Scheme 1. Graphic illustration of the phosphorescence-IDA. (a) The indicator (upper row), porphyrin linked to E1 or E2 (middle row), has long phosphorescence lifetime (lower row). (b) Binding of the indicator to an antibody (upper and middle row) has quenching effect on the indicator phosphorescence lifetime (lower row). (c) An analyte is introduced into the system which replaces the indicator. (d) Dequenching of the indicator phosphorescence occurs.

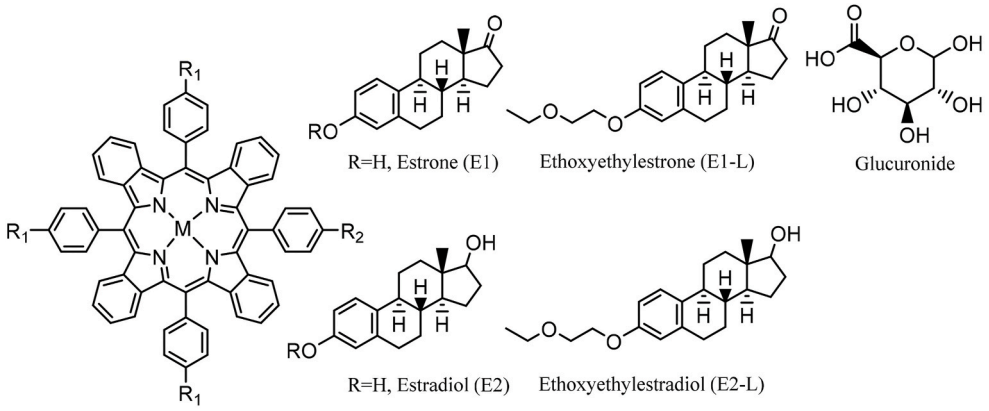

Compounds	R	R1	R2	M
E1S	SO_4H_2			
E1G	Glucuronide			
E2S	SO_4H_2			
E2G	Glucuronide			
TPTBP		H	H	-
Pd(TPTBP)		H	H	Pd
Pd(TPTBP-S4)		$SO_3^-Na^+$	$SO_3^-Na^+$	Pd
Por-COOH		$SO_3^-Na^+$	CO_2H	Pd
E1-Por	No R	$SO_3^-Na^+$	CO_2-estrone	Pd
E2-Por	No R	$SO_3^-Na^+$	CO_2-estradiol	Pd
E1-L-Por	No R	$SO_3^-Na^+$	CO_2-ethoxyethylestrone	Pd
E2-L-Por	No R	$SO_3^-Na^+$	CO_2-ethoxyethylestradiol	Pd

Scheme 2. Chemical structures of the tetrabenzoporphyrins and E1/E2 derivatives.

were soluble in water due to the presence of the negatively charged sulfonate groups. The absorption maxima were at λ_{max} ~440 nm (ε ~ 15000–42000) and 627 nm (ε ~ 6000–17000) (See Table 1). One can see that the absorption bands of TPTBP at ~440 nm and 627 nm are conserved even when estrone or estradiol are closely attached to the porphyrin skeleton as in E1-Por and E2-Por. When excited at 635 nm, Por-COOH emits at 804 nm. The relative emission intensities of all the compounds at different concentrations are listed in Table 1. They show some linearity at low concentrations and seem to diverge from linearity at higher concentrations (data not shown). This phenomenon is related to cluster formation by stacking of the planar multi-rings system of the porphyrins, which quenches the phosphorescence when above a critical concentration. The phosphorescence lifetimes of E1-L-Por and E2-L-Por (τ ~ 260 μs and 240 μs at 25 °C, respectively) are long enough. Together with the absorption efficacies, they indicate that these compounds are suitable labeled antigen analytes for immunosensing.

Since biological assays have to be performed at 37°C, there was a need to check whether the spectroscopic parameters are influenced by temperature. It is known that the fluorescence intensity in the emission spectra of tetraphenylporphyrin, as well as the emission lifetime, decrease with temperature increase. This property was used for thermal sensing [85]. Porphyrin dimers show similar spectroscopic response and, for this reason, were proposed for viscosity sensing [86]. The same effect on the emission bands was observed with the zinc porphyrin tweezer $(ZnTPP)_2$ in DSPC liposomes [87]. It is thought that the change in temperature brings about a change in the probabilities of radiative

Table 1
Absorption and emission data for the tetrabenzoporphyrin derivatives.

Compound (c = 6–8 mM in water)	Soret band λ_{max}	Q band λ	Temp °C	ε at λ 440 nm	ε at λ 627 nm	τ μs 10 ng/mL	Relative emission intensity at 804 nm (excitation at 635 nm) C (mg/mL)			
							0.002	0.005	0.01	0.02
Por-COOH	438.5	626	25	25900	15000	225				
E1-Por	438	625	25	42329	16475	232	706	756	1447	2356
			37	40823	15513	ND	504	825	1209	1984
			50	40464	15227	181	587	736	1181	1789
E2-Por	442	628	25	28136	10962	234	482	647	956	1800
			37	26861	10198	ND	511	635	916	1505
			50	26633	9947	186	449	588	842	1605
E1-L-Por	439	627	25	23758	9565	260	547	584	764	1368
			37	23198	9145	229	552	565	876	1138
			50	22520	8696	170	450	522	683	1202
E2-L-Por	439	626	25	15734	6713	240	397	533	716	1402
			37	14965	6292	220	565	595	769	1132
			50	14450	5929	182	459	512	584	947

*ND – not determined.

versus non-radiative transition [88]. Thereafter, we measured the spectroscopic parameters of tetrabenzoporphyrin derivatives (E1 or E2-Por, E1 or E2-L-Por) at three temperatures (25, 37 and 50°C) and four concentrations (0.002–0.02 mg/mL), and found that the relative emission intensity reflecting the quantum yield at 804 nm (excitation at 635 nm) decreases while temperature increases (Table 1). The opposite effects of thermal quenching (dominant) together with the disaggregation of the porphyrins aggregates can explain this phenomenon [85]. Moreover, the existence of tautomerism in the excited state was also reported, which can cause decrease of the signal intensities [89]. This decrease of the emission intensity at the incubation temperature (37 °C) as compared with room temperature (25°C) should not affect the detection capacity of the system since it is maintained in the same order of magnitude. For any of the tetrabenzoporphyrin derivatives (E1 or E2-Por, E1 or E2-L-Por), the absorption intensities of the Soret band and the Q band slightly decreased as the temperature increase (from 25 to 50°C), as shown by their extinction coefficients (Table 1). As a rule, the intensity of the Soret band is still bigger than the intensity of the Q band, however, the gap between them decreases while the temperature increases. Such a phenomenon has already been described [87,90].

Phosphorescence quenching by oxygen is a highly significant issue in the photophysical characteristics of porphyrins [91–95]. This was the basis for the development of oxygen sensors based on porphyrins. The influence of some cyclodextrins on the phosphorescent properties of some Pd-porphyrins had also been analyzed [96]. Enhancement of the phosphorescent signal of Pd (TPTBP-S_4) in the presence of met-β-cyclodextrin (τ 325–330 μs, at 795 nm in water) was also observed, probably because met-β-cyclodextrin protects the molecule against quenching by oxygen. These data shed light on the importance of the environment for the photophysical properties of an emitting system like Pd (TPTBP-S_4). In view of our findings, we could not ignore the bias that quenching by oxygen dissolved in water may have introduced into our measurements. We solved this problem by adding small amounts of sodium sulfite, an oxygen scavenger, to all the porphyrin conjugate solutions [97]. This method was already been used to avoid the phosphorescence quenching of monofunctional p-isothiocyanatophenyl derivatives of Pt (II)– and Pd(II)–coproporphyrin developed for protein labeling [98].

3.2. *Establishment of indirect competitive ELISA for E1/E2 and E1/E2-Por*

To determine if a specific antibody can be used as competitive receptor for some antigens, an indirect competitive ELISA was developed. To obtain the best spectrometric signal, some parameters such as concentration of the plate-coating antigen solutions and immunoassay blocking buffers were screened (data not shown) as were some special preparations of a polyclonal rabbit anti E2 and commercial anti E1 antibody. The sensitivity of the indirect competitive ELISA was evaluated using IC_{50} values (concentration of antigen that produced 50% inhibition). The specificity of the immunoassay was determined by adding various free competitors at different concentrations and letting them compete with the plate-coated antigen already bound to the antibody. For E2 antigens, an anti E2 polyclonal Ab was used. Although estradiol was our first choice as a competitive candidate, it was rejected due to its low water solubility. As mentioned above, the human body eliminates estrone and estradiol mainly as their sulfonated (E1S or E2S) or glucuronidated (E1G or E2G) metabolites. For this reason, E2S and E2G were selected as potential competitors. Their measured IC_{50} values are 0.4 and 10.5 ng/mL, respectively. The indirect competitive ELISA was also performed as reported above for the polyclonal rabbit anti E1, another capture antibody. E1G competes for binding to E1 antibody with an IC_{50} value of 71.4 ng/mL (Fig. 1) while a high IC_{50} value of 1482 ng/mL was obtained for its competition for the E2 antibody.

Using the same method, IC_{50} values were calculated for all competitors used to "challenge" both E1 and E2 antibodies. The values found for E1S, E1G, E2S and E2G correlate well with IC_{50} values reported in the literature [55,99,100]. As expected, the results showed that any E2 derivative is a better competitor for the E2 antibody than is any of E1 derivatives, while any E1 derivative is a better competitor for the E1 antibody than is any E2 derivative (Fig. 1). As a rule, the IC_{50} values obtained with all the estradiol derivatives are lower than those obtained for the estrone derivatives. When estrone is directly linked to the porphyrin skeleton (E1-Por), the IC_{50} values (5888 ng/mL) was higher, by more than 2 orders of magnitude than the IC_{50} values for E1S. When estradiol is directly linked to the porphyrin skeleton (E2-Por), the IC_{50} values (219 ng/mL) is higher by almost 3 orders of magnitude than the IC_{50} values for E2S.

At this point, we understood that our molecules are too small to measure binding constants via an indirect competitive method such as ELISA. We turned to the Octet platform which is a label-free analytical technology which was developed to obtain accurate information about rates of biomolecular complex formation and complex stability [101]. Because the results obtained were also unsatisfactory, we turned to SPR, one of the most advanced label free detection techniques for small molecules. SPR analysis is characterized by high sensitivity as well as the possibility of a real time read-out and direct measurement of binding kinetics. However, direct detection of small molecules by SPR is still very challenging due to their small size and, hence, their inadequate signal-to-noise ratios [102], so, direct SPR methods for small molecule detection using immunosensors may suffer from inadequate sensitivity [103]. The dissociation constant values are inconclusive, and interactions between E1-Por and E2-Por with the appropriate antibody were very weak so that SPR was unable to determine accurate K_D values. Since the K_{on} and K_{off} measured for E1-Por and E2-Por were too fast, only the steady state K_Ds were measured with value of less than 4 mM for both compounds (data not shown). In light of these disappointing results, it was clear that E1-Por and E2-Por are not suitable for the IDA in which a

a

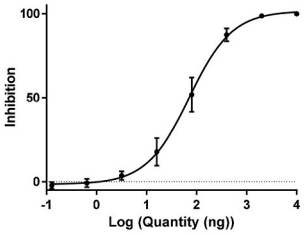

b

Compounds	Poly. Rabbit anti E1	Poly. Rabbit anti E2
E1G	71.4	1482
E1S	36.9	728.9
E2G	3609	10.5
E2S	14,943	0.4
E1-Por	5888	4314
E2-Por	18,163	219
E1-L-Por	424	NA
E2-L-Por	NA	23.5

*NA - not applicable

Fig. 1. (a) Example of an inhibition curve of E1G and E1-Ab. (b) IC_{50} values (ng/mL) of compounds in E1/E2 immunoassay.

strong binding of the analyte is needed. As was already suspected, the reason for the weak binding of E1-Por and E2-Por is the proximity of the porphyrin skeleton to the steroid structures of estrone and estradiol, resulting in significant steric hindrance to the approach to the antibody active site.

We assumed that labeled molecules in which the estrone or estradiol are attached to the porphyrin through a linker would be more suitable. The choice of the linker was important since, if too long, the porphyrin chromophore will not "sense" the presence of the antibody at all so that the needed effect of extinction would not occur. As already stated, we choose to introduce an ethylene glycol chain which seemed to have a proper length and is also sufficiently hydrophilic to maintain water-solubility. As expected, the binding affinities obtained with E1 or E2 attached to the porphyrin skeleton through this linker were more encouraging. E2-L-Por is a good competitor of E2S and E2G with an IC_{50} value of 23.5 ng/mL against Poly. Rabbit anti E2 and the IC_{50} value for E1-L-Por is 424 ng/mL against Poly. Rabbit anti E1. These results illustrate the importance of designing compounds in which the estrone or estradiol moiety keeps a high degree of freedom as in E1-L-Por and E2-L-Por. These competitors are at least 10 times better than the E1-Por and E2-Por derivatives. The structures of E1-L-Por and E2-L-Por allow a relatively easy access of E1 and E2 to the antibodies' binding sites, because the ethoxyethyl linker pushes the bulky tetrabenzoporphyrin out of the way.

3.3. The spectrophotometric device

Several groups have reported on the development of devices designed for phosphorescence lifetime measurements. For example, an optimized time resolved fluorescence reader was used for the detection of proteins bound to porphyrins [98,104]. We used a spectrophotometric device which is a phosphorescence decay time reader that was developed to detect the presence of small quantities of an analyte (i.e. estradiol, estrone) [105]. In such use, it contains a light emitter, a detector configured to detect light emitted from an indicator molecule, a device body configured to hold the sample, and a controller configured to analyze a change in the emission frequency/emission lifetime of the indicator (see Fig. 2). This device possesses a reader system configured to provide a non-invasive, high speed (1 s or less), automated measurement of an analyte's signal. The system measures luminescent lifetime from an indicator molecule with an expected lifetime range of ~100–~300 μs as is typical for porphyrin-based indicators. Although short lifetime (nanoseconds) NIR chromophores at other wavelengths such as visible range are also configurable with this device, though chromophores with longer lifetimes (microseconds) NIR are preferred. The optical design allows the excitation of an indicator molecule from four optical sensing modules or pods containing a total of eight 630 nm LEDS pulsed simultaneously, with a return signal captured from four silicon photomultiplier chips detectors (SiPM). The concentration of the

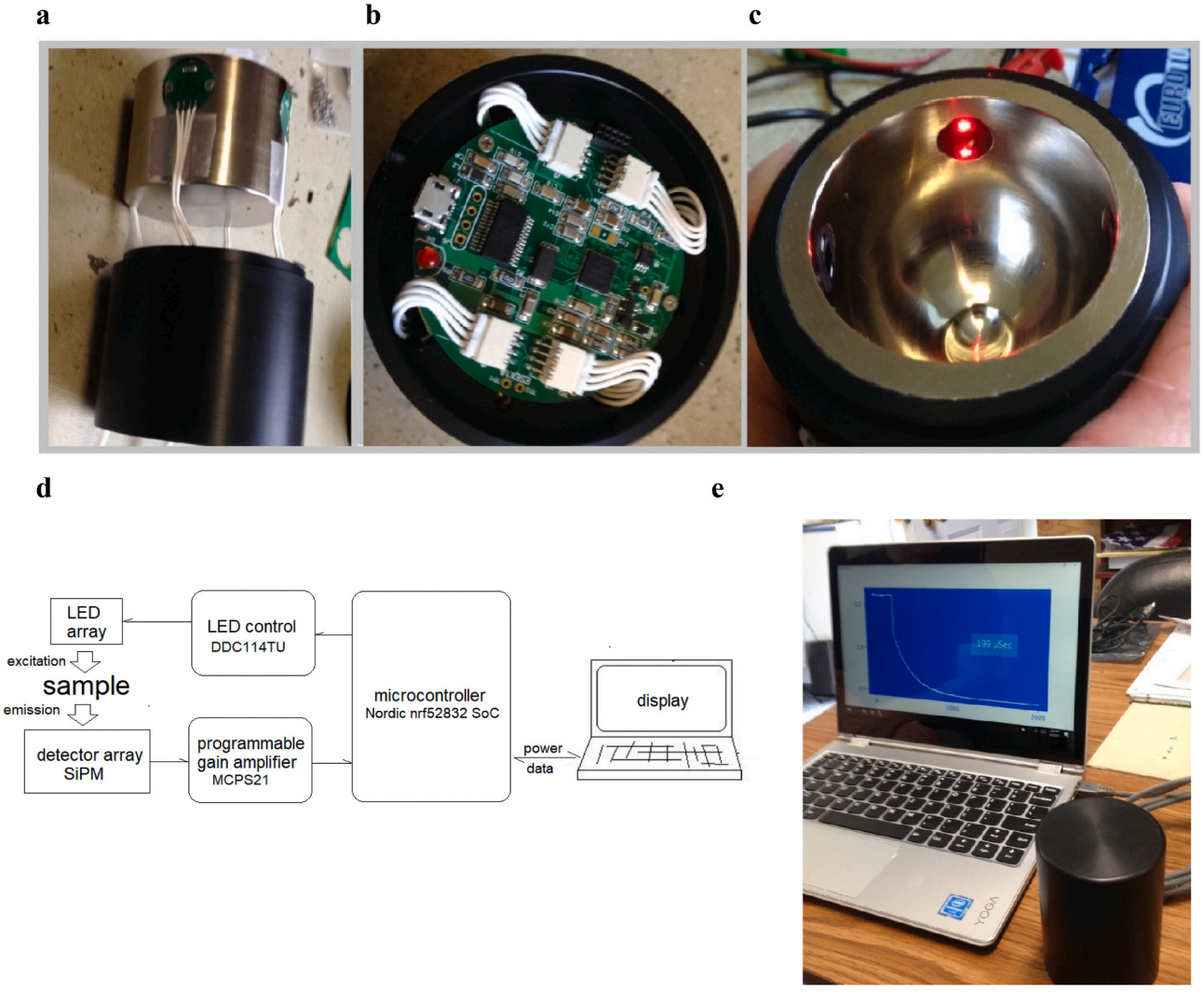

Fig. 2. The optical device. (a) Optical pods with reflective inner sphere. (b) Central microcontroler NRF52832. (c) Polished inner chamber contained within a light tight black Delrin encasement. (d) Block diagram of the optical device. (e) Laptop console with lifetime decay display.

analyte is a function of the decay time. An advantage of this device is its small size and low weight, and its capacity to detect small amounts (picograms) of analyte bound to an indicator even through a transparent membrane or peel.

3.4. Quenching assay

Results from the indirect competitive ELISA has led to the conclusion that the tetrabenzoporphyrin derivatives E1-L-Por and E2-L-Por are good competitors of the E1 and E2 natural derivatives, when using Poly. Rabbit anti E1 and E2 antibodies, respectively. Since we were interested in developing of a 17β-estradiol detection method, an optical immunosensor IDA-based system using the phosphorescence of E2-L-Por for optical sensing was settled upon (see Scheme 1). First, phosphorescence lifetime measurements were performed using an extremely sensitive, miniaturized, and portable optical reader that can determine decay times of luminescent compounds like tetrabenzoporphyrins at exceptionally low concentrations. Values of τ 232, 234, 260, and 240 μs for E1-Por, E2-Por, E1-L-Por, and E2-L-Por, respectively were obtained in concentrations range below 6 nM. Second, as already stated, the quenching of the phosphorescence of E2-L-Por following its specific binding to the antibody was established. Finally, estradiol and E2-L-Por compete at the antibody binding site, and E2S or E2G displaces E2-L-Por, giving rise to an optical signal due to the recovery of the quenched phosphorescence.

In this experimental setting, E2-L-Por (30 fmol) was allowed to bind to a specific antibody. A rapid decrease, down to 100% quenching, in the phosphorescence decay time, occurred from τ = 220 μs–0 μs (Fig. 3A and B). When E2S (2 μg/mL) was added, a full phosphorescence recovery occurred (τ = 218 μs, Fig. 3C and D). In the same manner, E1-L-Por (30 fmol) was also fully quenched from τ = 229 μs–0 μs, and after E1S was added, a full phosphorescence recovery was measured (τ = 226 μs, Fig. 3D).

These studies show that the IDA based optical immunosensor that we developed gives an excellent signal when the analyte (E1S/E2S) displaces the indicator (E1-L-Por/E2-L-Por), for which affinity to the specific antibody is lower. This was enabled by the cross-reactivity between those two analytes. As shown, cross-reactivity between different analytes occurs since the specific antibody which was raised against one specific antigen (E2) binds to a variety of analytes (Fig. 1). Our choice of emission lifetime measurement instead of emission intensity creates an opportunity for the use of this method in countless other biological preparations. Fluorescence/phosphorescence lifetime measurements have the important advantage of being independent of the local fluorophore concentration. Since the lifetime is influenced by the fluorophore microenvironment, high sensitivity can be expected.

4. Conclusion

New porphyrin palladium-tetraphenyltetrabenzoporphyrin derivatives were designed and used in the present work: E1-Por, E2-Por, E1-L-Por and E2-L-Por, to develop an IDA based optical immunosensor. Their IC_{50} values (Fig. 1) show that they are recognized by the polyclonal rabbit antibodies Ab-E1 and Ab-E2. As expected, the derivatives that include a linker (E1-L-Por and E2-L-Por) are better ligands than their more compact analogs (E1-Por and E2-Por). They are easily displaced by the endogenous antigens (E1S, E2S, E1G and E2G). Most importantly, the phosphorescence of the labeled antigens, E1-L-Por and E2-L-Por, is quenched following their binding to the proper antibody, and their phosphorescence lifetime, measured with a novel spectrophotometric device, is restored following displacement from the antibody active site by the endogenous antigens. This radical switch-off/switch-on process defines E1-L-Por and E2-L-Por as strong candidates for *in vivo* and *in vitro* immunosensing of estrone and 17β-estradiol.

Authors' contributions

Arik Monash, Methodology. Writing – review & editing, Writing – original draft, Visualization, Formal analysis. Daniele Marciano, Writing – review & editing. Visualization, Formal analysis, Methodology. Conceptualization, Supervision. Arthur (Skip) Colvin, Software. Validation. Writing – review & editing, Rafi Fass, Conceptualization,

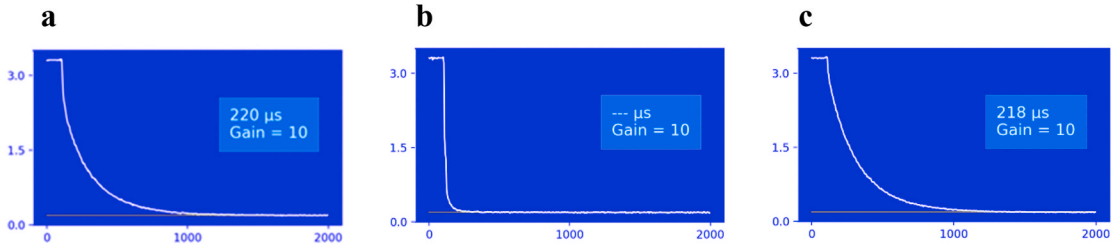

d

Compounds (30 fmol)	τ (μs)	Specific Ab (nmole)	τ after adding specific Ab (μs)	τ recovery after adding 2μg/mL E1S or E2S (μs)
E1-L-Por	229	3.6	0	226
E2-L-Por	220	180	0	218

Fig. 3. (a) Phosphorescence decay time of the indicator. (b) Phosphorescence decay time of the indicator after binding to its specific Ab. (c) Phosphorescence decay time of the indicator after addition of competitive analyte. (d) Phosphorescence decay time values (μs) of E1-L-Por *vs* E2-L-Por in a quenching assay using the optical immunosensor.

Methodology. Project administration, Yair Dvash, Methodology. Project administration, Osnat Rosen, Conceptualization. Validation. Writing – review & editing, Writing – original draft, Visualization, Methodology, Supervision, Project administration, Visualization, Formal analysis.

Declaration of competing interest

The authors declare that they have no known competing financial interests or personal relationships that could have appeared to influence the work reported in this paper.

References

[1] P. Fechner, O. Bleher, M. Ewald, K. Freudenberger, D. Furin, U. Hilbig, F. Kolarov, K. Krieg, L. Leidner, G. Markovic, G. Proll, F. Pröll, S. Rau, J. Riedt, B. Schwarz, P. Weber, J. Widmaier, Size does matter! Label-free detection of small molecule-protein interaction, Anal. Bioanal. Chem. 406 (2014) 4033–4051, https://doi.org/10.1007/s00216-014-7834-4.

[2] R. Peltomaa, B. Glahn-Martínez, E. Benito-Peña, M.C. Moreno-Bondi, Optical biosensors for label-free detection of small molecules, Sensors 18 (2018), https://doi.org/10.3390/s18124126.

[3] A. Vasilescu, C. Polonschii, A.M. Titoiu, R. Mishra, S. Peteu, J.-L. Marty, Bioassays and biosensors for food analysis. Commer. Biosens. Their Appl., Elsevier, 2020, pp. 217–258, https://doi.org/10.1016/b978-0-12-818592-6.00009-8.

[4] N. Verma, A. Bhardwaj, Biosensor technology for pesticides-A review electrochemical biosensor view project desulphurization view project, Artic. Appl. Biochem. Biotechnol. 175 (2015) 3093–3119, https://doi.org/10.1007/s12010-015-1489-2.

[5] W. Jawaid, K. Campbell, K. Melville, S.J. Holmes, J. Rice, C.T. Elliott, Development and validation of a novel lateral flow immunoassay (LFIA) for the rapid screening of paralytic shellfish toxins (PSTs) from shellfish extracts, Anal. Chem. 87 (2015) 5324–5332, https://doi.org/10.1021/acs.analchem.5b00608.

[6] Y. Nie, Y. Teng, P. Li, W. Liu, Q. Shi, Y. Zhang, Label-free aptamer-based sensor for specific detection of malathion residues by surface-enhanced Raman scattering, Spectrochim. Acta Part A Mol. Biomol. Spectrosc. 191 (2018) 271–276, https://doi.org/10.1016/j.saa.2017.10.030.

[7] F.S. Ligler, Perspective on optical biosensors and integrated sensor systems, Anal. Chem. 81 (2009) 519–526, https://doi.org/10.1021/ac8016289.

[8] D.R. Shankaran, K.V. Gobi, N. Miura, Recent advancements in surface plasmon resonance immunosensors for detection of small molecules of biomedical, food and environmental interest, Sensor. Actuator. B Chem. 121 (2007) 158–177, https://doi.org/10.1016/j.snb.2006.09.014.

[9] D.R. Shankaran, T. Kawaguchi, S.J. Kim, K. Matsumoto, K. Toko, N. Miura, Evaluation of the molecular recognition of monoclonal and polyclonal antibodies for sensitive detection of 2,4,6-trinitrotoluene (TNT) by indirect competitive surface plasmon resonance immunoassay, Anal. Bioanal. Chem. 386 (2006) 1313–1320, https://doi.org/10.1007/s00216-006-0699-4.

[10] N. Adányi, I.A. Levkovets, S. Rodriguez-Gil, A. Ronald, M. Váradi, I. Szendro, Development of immunosensor based on OWLS technique for determining Aflatoxin B1 and Ochratoxin A, Biosens. Bioelectron. 22 (2007) 797–802, https://doi.org/10.1016/j.bios.2006.02.015.

[11] B.J. Yakes, K.M. Kanyuck, S.L. DeGrasse, First report of a direct surface plasmon resonance immunosensor for a small molecule seafood toxin, Anal. Chem. 86 (2014) 9251–9255, https://doi.org/10.1021/ac502271y.

[12] X.H. Fu, Surface plasmon resonance immunoassay for Ochratoxin A based on nanogold hollow balls with dendritic surface, Anal. Lett. 40 (2007) 2641–2652, https://doi.org/10.1080/00032710701588366.

[13] P. Boltovets, S. Shinkaruk, L. Vellutini, B. Snopok, Self-tuning interfacial architecture for Estradiol detection by surface plasmon resonance biosensor, Biosens. Bioelectron. 90 (2017) 91–95, https://doi.org/10.1016/j.bios.2016.11.017.

[14] S. Joshi, R.M. Annida, H. Zuilhof, T.A. Van Beek, M.W.F. Nielen, Analysis of mycotoxins in beer using a portable nanostructured imaging surface plasmon resonance biosensor, J. Agric. Food Chem. 64 (2016) 8263–8271, https://doi.org/10.1021/acs.jafc.6b04106.

[15] A. Al-Jawdah, A. Nabok, R. Jarrah, A. Holloway, A. Tsargorodska, E. Takacs, A. Szekacs, Mycotoxin biosensor based on optical planar waveguide, Toxins 10 (2018), https://doi.org/10.3390/toxins10070272.

[16] J.H. Park, J.Y. Byun, H. Mun, W.B. Shim, Y.B. Shin, T. Li, M.G. Kim, A regeneratable, label-free, localized surface plasmon resonance (LSPR) aptasensor for the detection of ochratoxin A, Biosens. Bioelectron. 59 (2014) 321–327, https://doi.org/10.1016/j.bios.2014.03.059.

[17] B.C. Galarreta, M. Tabatabaei, E. Peyrin, Microfluidic channel with embedded SERS 2D platform for the aptamer detection of ochratoxin A Antivenom production View project Nanoscale Printing of electronics and sensors View project, Artic. Anal. Bioanal. Chem. 405 (2012) 1613–1621, https://doi.org/10.1007/s00216-012-6557-7.

[18] T.E. Rohr, T. Cotton, N. Fan, P.J. Tarcha, Immunoassay employing surface-enhanced Raman spectroscopy, Anal. Biochem. 182 (1989) 388–398, https://doi.org/10.1016/0003-2697(89)90613-1.

[19] S. Pang, T. Yang, L. He, Review of surface enhanced Raman spectroscopic (SERS) detection of synthetic chemical pesticides, TrAC Trends Anal. Chem. (Reference Ed.) 85 (2016) 73–82, https://doi.org/10.1016/j.trac.2016.06.017.

[20] T. Kamra, C. Xu, L. Montelius, J. Schnadt, S.A. Wijesundera, M. Yan, L. Ye, Photoconjugation of molecularly imprinted polymer nanoparticles for surface-enhanced Raman detection of propranolol, ACS Appl. Mater. Interfaces 7 (2015) 27479–27485, https://doi.org/10.1021/acsami.5b09500.

[21] X. Zhou, F. Zhou, H. Liu, L. Yang, J. Liu, Assembly of polymer-gold nanostructures with high reproducibility into a monolayer film SERS substrate with 5 nm gaps for pesticide trace detection, Analyst 138 (2013) 5832–5838, https://doi.org/10.1039/c3an00914a.

[22] H. Zhang, W. Li, H. Luo, G. Xiong, Y. Yu, Quantitative determination of testosterone levels with biolayer interferometry, Chem. Biol. Interact. 276 (2017) 141–148, https://doi.org/10.1016/j.cbi.2017.05.013.

[23] V.C. Özalp, Dual-polarization interferometry for quantification of small molecules using aptamers, Anal. Bioanal. Chem. 402 (2012) 799–804, https://doi.org/10.1007/s00216-011-5499-9.

[24] K. Campbell, R. O'kennedy, C. Elliott, An evaluation of the capability of a biolayer interferometry biosensor to detect low-molecular-weight food contaminants, Artic. Anal. Bioanal. Chem. 405 (2013) 2535–2544, https://doi.org/10.1007/s00216-012-6677-0.

[25] B. Chocarro-Ruiz, S. Herranz, A. Fernández Gavela, J. Sanchís, M. Farré, M. P. Marco, L.M. Lechuga, Interferometric nanoimmunosensor for label-free and real-time monitoring of Irgarol 1051 in seawater, Biosens. Bioelectron. 117 (2018) 47–52, https://doi.org/10.1016/j.bios.2018.05.044.

[26] T. Chalyan, R. Guider, L. Pasquardini, M. Zanetti, F. Falke, E. Schreuder, R. G. Heideman, C. Pederzolli, L. Pavesi, Asymmetric Mach-Zehnder interferometer based biosensors for Aflatoxin M1 detection, Biosensors 6 (2016), https://doi.org/10.3390/bios6010001.

[27] M. Sanders, D. McPartlin, K. Moran, Y. Guo, M. Eeckhout, R. O'Kennedy, S. De Saeger, C. Maragos, Comparison of Enzyme-linked Immunosorbent assay, surface plasmon resonance and biolayer interferometry for screening of deoxynivalenol in Wheat and Wheat Dust, Toxins 8 (2016), https://doi.org/10.3390/toxins8040103.

[28] S. Rau, G. Gauglitz, Reflectometric interference spectroscopy (RIfS) as a new tool to measure in the complex matrix milk at low analyte concentration, Anal. Bioanal. Chem. 402 (2012) 529–536, https://doi.org/10.1007/s00216-011-5470-9.

[29] S. Akter, M. Vehniäinen, L. Spoof, S. Nybom, J. Meriluoto, U. Lamminmäki, Broad-spectrum noncompetitive immunocomplex immunoassay for cyanobacterial peptide hepatotoxins (microcystins and nodularins), Anal. Chem. 88 (2016) 10080–10087, https://doi.org/10.1021/acs.analchem.6b02470.

[30] A. Nabok, A.M. Al-Jawdah, A. Tsargorodska, Development of planar waveguide-based immunosensor for detection of low molecular weight molecules such as mycotoxins, Sensor. Actuator. B Chem. 247 (2017) 975–980, https://doi.org/10.1016/j.snb.2017.01.197.

[31] C. Pacholski, L.A. Perelman, M.S. Vannieuwenhze, M.J. Sailor, Small molecule detection by reflective interferometric Fourier transform spectroscopy (RIFTS), Phys. Status Solidi Appl. Mater. Sci. 206 (2009) 1318–1321, https://doi.org/10.1002/pssa.200881072.

[32] N. Bhalla, P. Jolly, N. Formisano, P. Estrela, Introduction to biosensors, Essays Biochem. 60 (2016) 1–8, https://doi.org/10.1042/EBC20150001.

[33] J. Rainbow, E. Sedlackova, S. Jiang, G. Maxted, D. Moschou, L. Richtera, P. Estrela, Integrated electrochemical biosensors for detection of waterborne pathogens in low-resource settings, Biosensors 10 (2020), https://doi.org/10.3390/bios10040036.

[34] I.H. Cho, J. Lee, J. Kim, M.S. Kang, J.K. Paik, S. Ku, H.M. Cho, J. Irudayaraj, D. H. Kim, Current technologies of electrochemical immunosensors: perspective on signal amplification, Sensors (2018) 18, https://doi.org/10.3390/s18010207.

[35] A.A. Lahcen, A. Amine, Recent Advances in Electrochemical Sensors Based on Molecularly Imprinted Polymers and Nanomaterials, vol. 31, Wiley Online Libr, 2018, pp. 188–201, https://doi.org/10.1002/elan.201800623.

[36] K. Ikebukuro, C. Kiyohara, K. Sode, Novel electrochemical sensor system for protein using the aptamers in sandwich manner. Biosens. Bioelectron., Elsevier Ltd, 2005, pp. 2168–2172, https://doi.org/10.1016/j.bios.2004.09.002.

[37] J. Lee, W. Yoshida, K. Abe, K. Nakabayashi, H. Wakeda, K. Hata, C.A. Marquette, L.J. Blum, K. Sode, K. Ikebukuro, Development of an electrochemical detection system for measuring DNA methylation levels using methyl CpG-binding protein and glucose dehydrogenase-fused zinc finger protein, Biosens. Bioelectron. 93 (2017) 118–123, https://doi.org/10.1016/j.bios.2016.09.060.

[38] C. Cristea, A. Florea, M. Tertis, R. Sandulescu, Immunosensors, Biosens. - Micro Nanoscale Appl, InTech, 2015, https://doi.org/10.5772/60524.

[39] J. Homola, Surface plasmon resonance sensors for detection of chemical and biological species, Chem. Rev. 108 (2008) 462–493, https://doi.org/10.1021/cr068107d.

[40] B.T. Nguyen, E.V. Anslyn, Indicator–displacement assays, Coord. Chem. Rev. 250 (2006) 3118–3127, https://doi.org/10.1016/j.ccr.2006.04.009.

[41] B.T. Nguyen, S.L. Wiskur, E.V. Anslyn, Using indicator-displacement assays in test strips and to follow reaction kinetics, Org. Lett. 6 (2004) 2499–2501, https://doi.org/10.1021/ol0493599.

[42] S.L. Wicks, A.E. Hargrove, Fluorescent indicator displacement assays to identify and characterize small molecule interactions with RNA, Methods 167 (2019) 3–14, https://doi.org/10.1016/j.ymeth.2019.04.018.

[43] A. Murata, Y. Harada, T. Fukuzumi, K. Nakatani, Fluorescent indicator displacement assay of ligands targeting 10 microRNA precursors, Bioorg. Med. Chem. 21 (2013) 7101–7106, https://doi.org/10.1016/j.bmc.2013.09.007.

[44] J. Zhang, S. Umemoto, K. Nakatani, Fluorescent indicator displacement assay for ligand-RNA interactions, J. Am. Chem. Soc. 132 (2010) 3660–3661, https://doi.org/10.1021/ja100089u.

[45] S. Umemoto, S. Im, J. Zhang, M. Hagihara, A. Murata, Y. Harada, T. Fukuzumi, T. Wazaki, S.I. Sasaoka, K. Nakatani, Structure-activity studies on the fluorescent indicator in a displacement assay for the screening of small molecules binding to RNA, Chem. Eur J. 18 (2012) 9999–10008, https://doi.org/10.1002/chem.201103932.

[46] A. Nascetti, M. Mirasoli, E. Marchegiani, M. Zangheri, F. Costantini, A. Porchetta, L. Iannascoli, N. Lovecchio, D. Caputo, G. de Cesare, S. Pirrotta, A. Roda, Integrated chemiluminescence-based lab-on-chip for detection of life markers in extraterrestrial environments, Biosens. Bioelectron. 123 (2019) 195–203, https://doi.org/10.1016/j.bios.2018.08.056.

[47] T. Minami, Y. Liu, A. Akdeniz, P. Koutnik, N.A. Esipenko, R. Nishiyabu, Y. Kubo, P. Anzenbacher, Intramolecular indicator displacement assay for anions: supramolecular sensor for glyphosate, J. Am. Chem. Soc. 136 (2014) 11396–11401, https://doi.org/10.1021/ja504535q.

[48] J. Chan, S.C. Dodani, C.J. Chang, Reaction-based small-molecule fluorescent probes for chemoselective bioimaging, Nat. Chem. 4 (2012) 973–984, https://doi.org/10.1038/nchem.1500.

[49] K.A. Franz, W.G. Kehr, A. Siggel, J. Wieczoreck, W. Adam, Luminescent materials. Ullmann's Encycl. Ind. Chem., Wiley-VCH Verlag GmbH & Co. KGaA, Weinheim, Germany, 2000, https://doi.org/10.1002/14356007.a15_519.

[50] R.R. de Haas, R.P.M. van Gijlswijk, E.B. van der Tol, J. Veuskens, H.E. van Gijssel, R.B. Tijdens, J. Bonnet, N.P. Verwoerd, H.J. Tanke, Phosphorescent platinum/palladium coproporphyrins for time-resolved luminescence microscopy, J. Histochem. Cytochem. 47 (1999) 183–196.

[51] M.M. Koskelin, A.E. Soini, N.J. Meltola, G.V. Ponomarev, Phosphorescent labeling reagents of platinum(II) and palladium(II) coproporphyrin-II. Preparation and performance characteristics, J. Porphyr. Phthalocyanines (2002), https://doi.org/10.1142/s108842460200066x.

[52] P.W. Zach, S.A. Freunberger, I. Klimant, S.M. Borisov, Electron-deficient near-infrared Pt(II) and Pd(II) benzoporphyrins with dual phosphorescence and unusually efficient thermally activated delayed fluorescence: first demonstration of simultaneous oxygen and temperature sensing with a single emitter, ACS Appl. Mater. Interfaces 9 (2017) 38008–38023, https://doi.org/10.1021/acsami.7b10669.

[53] D.B. Papkovsky, T.C. O'Riordan, Emerging applications of phosphorescent metalloporphyrins, J. Fluoresc. 15 (2005) 569–584, https://doi.org/10.1007/s10895-005-2830-x.

[54] I. Ojeda, J. López-Montero, M. Moreno-Guzmán, B.C. Janegitz, A. González-Cortés, P. Yáñez-Sedeño, J.M. Pingarrón, Electrochemical immunosensor for rapid and sensitive determination of estradiol, Anal. Chim. Acta 743 (2012) 117–124, https://doi.org/10.1016/j.aca.2012.07.002.

[55] X. Wang, L. Cohen, J. Wang, D.R. Walt, Competitive immunoassays for the detection of small molecules using single molecule arrays, J. Am. Chem. Soc. 140 (2018) 18132–18139, https://doi.org/10.1021/jacs.8b11185.

[56] Z. Liu, M. Hu, Natural polyphenol disposition via coupled metabolic pathways, Expet Opin. Drug Metabol. Toxicol. 3 (2007) 389–406, https://doi.org/10.1517/17425255.3.3.389.

[57] A. Stopforth, C.J. Grobbelaar, A.M. Crouch, P. Sandra, Quantification of testosterone and epitestosterone in human urine samples by stir bar sorptive extraction - thermal desorption - gas chromatography/mass spectrometry: application to HIV-positive urine samples, J. Separ. Sci. 30 (2007) 257–265, https://doi.org/10.1002/jssc.200600280.

[58] M. Kawaguchi, R. Ito, N. Sakui, N. Okanouchi, K. Saito, H. Nakazawa, Dual derivatization-stir bar sorptive extraction-thermal desorption-gas chromatography-mass spectrometry for determination of 17β-estradiol in water sample, J. Chromatogr. A (2006) 140–147, https://doi.org/10.1016/j.chroma.2005.06.088.

[59] H. Guo, K. Liu, Y. Liu, B. Fang, M. Liu, L. He, Z. Zeng, Molecularly imprinted solid-phase extraction for the selective determination of valnemulin in feeds with high performance liquid chromatography, J. Chromatogr. B Anal. Technol. Biomed. Life Sci. 879 (2011) 181–185, https://doi.org/10.1016/j.jchromb.2010.11.041.

[60] L. Havlíková, L. Nováková, L. Matysová, J. Šícha, P. Solich, Determination of estradiol and its degradation products by liquid chromatography, J. Chromatogr., A 1119 (2006) 216–223, https://doi.org/10.1016/j.chroma.2006.01.085.

[61] X. Liu, D.K.Y. Wong, Electrocatalytic detection of estradiol at a carbon nanotube|Ni(Cyclam) composite electrode fabricated based on a two-factorial design, Anal. Chim. Acta 594 (2007) 184–191, https://doi.org/10.1016/j.aca.2007.05.043.

[62] B. Salc, I. Biryol, Voltammetric investigation of β-estradiol, J. Pharmaceut. Biomed. Anal. 28 (2002) 753–759, https://doi.org/10.1016/S0731-7085(01)00676-8.

[63] B. Piro, S. Shi, S. Reisberg, V. Noël, G. Anquetin, Comparison of electrochemical immunosensors and aptasensors for detection of small organic molecules in environment, food safety, clinical and public security, Biosensors 6 (2016), https://doi.org/10.3390/bios6010007.

[64] B. Zhu, O.A. Alsager, S. Kumar, J.M. Hodgkiss, J. Travas-Sejdic, Label-free electrochemical aptasensor for femtomolar detection of 17β-estradiol, Biosens. Bioelectron. 70 (2015) 398–403, https://doi.org/10.1016/j.bios.2015.03.050.

[65] K.J. Huang, Y.J. Liu, G.W. Shi, X.R. Yang, Y.M. Liu, Label-free aptamer sensor for 17β-estradiol based on vanadium disulfide nanoflowers and Au nanoparticles, Sensor. Actuator. B Chem. 201 (2014) 579–585, https://doi.org/10.1016/j.snb.2014.05.055.

[66] N. Chaisuwan, H. Xu, G. Wu, J. Liu, A highly sensitive differential pulse anodic stripping voltammetry for determination of 17B-estradiol (E2) using CdSe quantum dots based on indirect competitive immunoassay, Biosens. Bioelectron. 46 (2013) 150–154, https://doi.org/10.1016/j.bios.2013.02.041.

[67] M.J. Monerris, F.J. Arévalo, H. Fernández, M.A. Zon, P.G. Molina, Development of a very sensitive electrochemical immunosensor for the determination of 17β-estradiol in bovine serum samples, Sensor. Actuator. B Chem. 208 (2015) 525–531, https://doi.org/10.1016/j.snb.2014.11.048.

[68] D. Vega, L. Agüí, A. González-Cortés, P. Yáñez-Sedeño, J.M. Pingarrón, Electrochemical detection of phenolic estrogenic compounds at carbon nanotube-modified electrodes, Talanta 71 (2007) 1031–1038, https://doi.org/10.1016/j.talanta.2006.05.071.

[69] J. Piwowarska, S. Radowicki, J. Pachecka, Simultaneous determination of eight estrogens and their metabolites in serum using liquid chromatography with electrochemical detection, Talanta 81 (2010) 275–280, https://doi.org/10.1016/j.talanta.2009.11.069.

[70] P.M. Ndangili, A.M. Jijana, P.G.L. Baker, E.I. Iwuoha, 3-Mercaptopropionic acid capped ZnSe quantum dot-cytochrome P450 3A4 enzyme biotransducer for 17β-estradiol, J. Electroanal. Chem. 653 (2011) 67–74, https://doi.org/10.1016/j.jelechem.2010.12.029.

[71] Y.S. Kim, H.S. Jung, T. Matsuura, H.Y. Lee, T. Kawai, M.B. Gu, Electrochemical detection of 17β-estradiol using DNA aptamer immobilized gold electrode chip, Biosens. Bioelectron. 22 (2007) 2525–2531, https://doi.org/10.1016/j.bios.2006.10.004.

[72] Z. Lin, L. Chen, G. Zhang, Q. Liu, B. Qiu, Z. Cai, G. Chen, Label-free aptamer-based electrochemical impedance biosensor for 17β-estradiol, Analyst 137 (2012) 819–822, https://doi.org/10.1039/c1an15856b.

[73] P.B. Eriksen, New extraction method for radioimmunoassay of serum estradiol, Clin. Chem. 27 (1981) 1926–1928, https://doi.org/10.1093/clinchem/27.11.1926.

[74] R. Mertens, R.J. Liedtke, J.D. Batjer, Evaluation of a radioimmunoassay for estradiol in unextracted serum, Clin. Chem. 29 (1983) 1961–1963, https://doi.org/10.1093/clinchem/29.11.1961.

[75] K. Tamate, M. Charleton, J.P. Gosling, D. Egan, M. Ishikawa, P.F. Fottrell, M. M. Kane, Direct colorimetric monoclonal antibody enzyme immunoassay for estradiol-17β in saliva, Clin. Chem. 43 (1997) 1159–1164, https://doi.org/10.1093/clinchem/43.7.1159.

[76] F. Dancoine, G. Couplet, J. Buvat, C. Guittard, G. Marcolin, J.C. Fourlinnie, Analytical and clinical evaluation of the Immulite® estradiol assay in serum from patients undergoing in vitro fertilization: estradiol increase in mature follicles, Clin. Chem. 43 (1997) 1165–1171, https://doi.org/10.1093/clinchem/43.7.1165.

[77] T.B. Xin, S.X. Liang, X. Wang, H. Li, J.M. Lin, Determination of estradiol in human serum using magnetic particles-based chemiluminescence immunoassay, Anal. Chim. Acta 627 (2008) 277–284, https://doi.org/10.1016/j.aca.2008.08.020.

[78] K. Majima, T. Fukui, J. Yuan, G. Wang, K. Matsumoto, Quantitative measurement of 17β-estradiol and estriol in river water by time-resolved fluoroimmunoassay, Anal. Sci. 18 (2002) 869–874, https://doi.org/10.2116/analsci.18.869.

[79] D.A. James, N. Swamy, N. Paz, R.N. Hanson, R. Ray, Synthesis and estrogen receptor binding affinity of a porphyrin- estradiol conjugate for targeted photodynamic therapy of cancer, Bioorg. Med. Chem. Lett 9 (1999) 2379–2384, https://doi.org/10.1016/S0960-894X(99)00390-X.

[80] D.L. Eastwood, M. Gouterman, Porphyrins. XVIII. Luminescence of (Co), (Ni), Pd, Pt complexes, J. Mol. Spectrosc. 35 (1970) 359–375, https://doi.org/10.1016/0022-2852(70)90179-7.

[81] S.A. Vinogradov, D.F. Wilson, Metallotetrabenzoporphyrins. New phosphorescent probes for oxygen measurements, J. Chem. Soc. Perkin Trans. 2 (1995) 103–111, https://doi.org/10.1039/p29950000103.

[82] O.S. Finikova, A.V. Cheprakov, S.A. Vinogradov, Synthesis and luminescence of soluble meso-unsubstituted tetrabenzo- and tetranaphtho[2,3]porphyrins, J. Org. Chem. 70 (2005) 9562–9572, https://doi.org/10.1021/jo051580r.

[83] A.Y. Lebedev, M.A. Filatov, A.V. Cheprakov, S.A. Vinogradov, Effects of structural deformations on optical properties of tetrabenzoporphyrins: free-bases and Pd complexes, J. Phys. Chem. 112 (2008) 7723–7733, https://doi.org/10.1021/jp8043626.

[84] J.S. Lindsey, S. Prathapan, T.E. Johnson, R.W. Wagner, Porphyrin building blocks for modular construction of bioorganic model systems, Tetrahedron 50 (1994) 8941–8968, https://doi.org/10.1016/S0040-4020(01)85364-3.

[85] I.E. Kolesnikov, A.A. Kalinichev, M.A. Kurochkin, E.Y. Kolesnikov, E. Lähderanta, Porphyrins as efficient ratiometric and lifetime-based contactless optical thermometers, Mater. Des. 184 (2019) 108188, https://doi.org/10.1016/j.matdes.2019.108188.

[86] A. Vyšniauskas, D. Ding, M. Qurashi, I. Boczarow, M. Balaz, H.L. Anderson, M. K. Kuimova, Tuning the sensitivity of fluorescent porphyrin dimers to viscosity and temperature, Chemistry 23 (2017), https://doi.org/10.1002/chem.201700740.

[87] J.R. Widom, W. Lee, A. Perdomo-Ortiz, D. Rappoport, T.F. Molinski, A. Aspuru-Guzik, A.H. Marcus, Temperature-dependent conformations of a membrane supported zinc porphyrin tweezer by 2D fluorescence spectroscopy, J. Phys. Chem. 117 (2013) 6171–6184, https://doi.org/10.1021/jp400394z.

[88] B.G. Evale, S.M. Hanagodimath, M. V Kulkarni, Effect of temperature on the fluorescence emission of 2H-chromen-2-one derivative in non-polar and polar solvents, J. Lumin. 130 (2010) 1325–1329, https://doi.org/10.1016/j.jlumin.2010.03.004.

[89] M. Uttamlal, A.S. Holmes-Smith, The excitation wavelength dependent fluorescence of porphyrins, Chem. Phys. Lett. 454 (2008) 223–228, https://doi.org/10.1016/j.cplett.2008.02.012.
[90] N.K. Giri, A. Banerjee, R.W.J. Scott, M.F. Paige, R.P. Steer, Spectroscopic and photophysical study of the demetallation of a zinc porphyrin and the aggregation of its free base in a tetraalkylphosphonium ionic liquid, Phys. Chem. Chem. Phys. 16 (2014) 26252–26260, https://doi.org/10.1039/c4cp04257c.
[91] P. Douglas, K. Eaton, Response characteristics of thin film oxygen sensors, Pt and Pd octaethylporphyrins in polymer films, Sensor. Actuator. B Chem. 82 (2002) 200–208, https://doi.org/10.1016/S0925-4005(01)01006-1.
[92] R.I. Dmitriev, H.M. Ropiak, G.V. Ponomarev, D.V. Yashunsky, D.B. Papkovsky, Cell-penetrating conjugates of coproporphyrins with oligoarginine peptides: rational design and application for sensing intracellular O2, Bioconjugate Chem. 22 (2011) 2507–2518, https://doi.org/10.1021/bc200324q.
[93] Y. Amao, K. Asai, I. Okura, H. Shinohara, H. Nishide, Platinum porphyrin embedded in poly(1-trimethylsilyl-1-propyne) film as an optical sensor for trace analysis of oxygen, Analyst 125 (2000) 1911–1914, https://doi.org/10.1039/b005838f.
[94] Y. Amao, Y. Tabuchi, Y. Yamashita, K. Kimura, Novel optical oxygen sensing material: metalloporphyrin dispersed in fluorinated poly(aryl ether ketone) films, Eur. Polym. J. 38 (2002) 675–681, https://doi.org/10.1016/S0014-3057(01)00235-X.
[95] M. Quaranta, S.M. Borisov, I. Klimant, Indicators for optical oxygen sensors, Bioanal. Rev. 4 (2012) 115–157, https://doi.org/10.1007/s12566-012-0032-y.
[96] A.P. Savitsky, A.V. Savitskaja, E.A. Lukjanetz, S.N. Dashkevich, E M, Makarova SPIE 2980 (1997), https://doi.org/10.1117/12.273533.short.
[97] K.H. Rashid, A.A. Khadom, Sodium sulfite as an oxygen scavenger for the corrosion control of mild steel in petroleum refinery wastewater: optimization, mathematical modeling, surface morphology and reaction kinetics studies, React. Kinet. Mech. Catal. 129 (2020) 1027–1046, https://doi.org/10.1007/s11144-020-01738-3.
[98] T.C. O'Riordan, A.E. Soini, D.B. Papkovsky, Monofunctional derivatives of coproporphyrins for phosphorescent labeling of proteins and binding assays, Anal. Biochem. 290 (2001) 366–375, https://doi.org/10.1006/abio.2001.4989.
[99] J. Duan, Z. Yuan, Development of an indirect competitive ELISA for ciprofloxacin residues in food animal edible tissues, J. Agric. Food Chem. 49 (2001) 1087–1089, https://doi.org/10.1021/jf000091j.
[100] W. Yin, J. Liu, T. Zhang, W. Li, W. Liu, M. Meng, F. He, Y. Wan, C. Feng, S. Wang, X. Lu, R. Xi, Preparation of monoclonal antibody for Melamine and development of an indirect competitive ELISA for Melamine detection in raw milk, milk powder, and animal feeds, J. Agric. Food Chem. 58 (2010) 8152–8157, https://doi.org/10.1021/jf1006209.
[101] R. Tobias, S. Kumaraswamy, Application note 14: biomolecular binding kinetics assays on the Octet platform, ForteBio a Div. Pall Life Sci. (2013) 1–66.
[102] B.J. Yakes, S. Prezioso, S.A. Haughey, K. Campbell, C.T. Elliott, S.L. Degrasse, An improved immunoassay for detection of saxitoxin by surface plasmon resonance biosensors, Sensor. Actuator. B Chem. 156 (2011) 805–811, https://doi.org/10.1016/j.snb.2011.02.043.
[103] M. Tomassetti, G. Merola, E. Martini, L. Campanella, G. Sanzò, G. Favero, F. Mazzei, Comparison between a direct-flow SPR immunosensor for ampicillin and a competitive conventional amperometric device: analytical features and possible applications to real samples, Sensors (2017) 17, https://doi.org/10.3390/s17040819.
[104] T.C. O'Riordan, A.E. Soini, J.T. Soini, D.B. Papkovsky, Performance evaluation of the phosphorescent porphyrin label: solid-phase immunoassay of α-fetoprotein, Anal. Chem. 74 (2002) 5845–5850, https://doi.org/10.1021/ac020346n.
[105] A.E. Colvin, US Patent App. 16/487, U. 2020, DEVICES and METHODS for DETERMINING ANALYTES, Freepatentsonline.Com2018 ,.. https://www.freepatentsonline.com/y2020/0229402.html.